Simulation and Optimization of HIT Solar Cells with Intrinsic Thin Amorphous Si Layer

Darko Bjelopavlić[1], Sanja Aleksić[1], Danijela Pantić[2], Branimir Đorđević[3] and Dragan Pantić[1]

Abstract – **Photovoltaic modules based on single crystal and polycrystalline silicon are almost 90% of the total world solar market, mainly because of its stable, robust and reliable characteristics. Therefore, great efforts are being made to improve their characteristics, especially their efficiency. One of the many approaches is HIT solar cells (hetero-junction solar cell with an intrinsic thin amorphous layer) fabricated at temperatures below 300°C. In this paper, the electrical characteristics of HIT solar cells are simulated by using the TCAD Silvaco software package. The structure of HIT solar cell is optimized in order to obtain their maximum efficiency.**

Keywords – **Solar cells, hetero-junction, amorphous/crystalline silicon, simulation, Silvaco.**

I. Introduction

Mono-crystalline, poly-crystalline and amorphous silicon solar cells are the most widely used group of the commercial solar cells. This is, primarily, based on the fact that these solar cells have stable characteristics over a long period of time, good reliability during operation, and their mass production, as developed in the microelectronics technology allows fast and relatively cheap production of solar cells based on silicon. The declining trend in the price of solar cells continues, and the technology improves so that the efficiency of solar cells produced becomes greater. One of the improvements is a combination of technologies based on single crystalline silicon (mono-crystalline silicon) layer with the addition of a thin amorphous layer. The resulting structure is known as HIT solar cell (hetero-junction with an amorphous intrinsic thin layer) produced by Sanyo Ltd., where the efficiency of commercially produced HIT solar cells is over 20%, and there is plenty of room for it to improve [1,2].

The production technologies of HIT solar cells use a thin intrinsic amorphous silicon layer (a-Si:H(i)) which is formed on both sides of wafer (Czochralski n-type c-Si), using low temperature PECVD process that takes place on 175°C or 250°C [3].In this way they avoid high temperature processes that degrade the interface surface of amorphous film and crystalline bulk. Thus obtained HIT structure has multiple advantages over the standard process. First, the width of a band gap Eg of amorphous silicon is in the range of 1.55eV to 1.87eV, which increases the efficiency at lower wavelengths, where is the most concentrated intensity of terrestrial solar radiation. Now, HIT structure shows better temperature characteristics, as well as a higher voltage V_{OC} (open-circuit voltage), because of a significant decrease in surface and interface recombination.

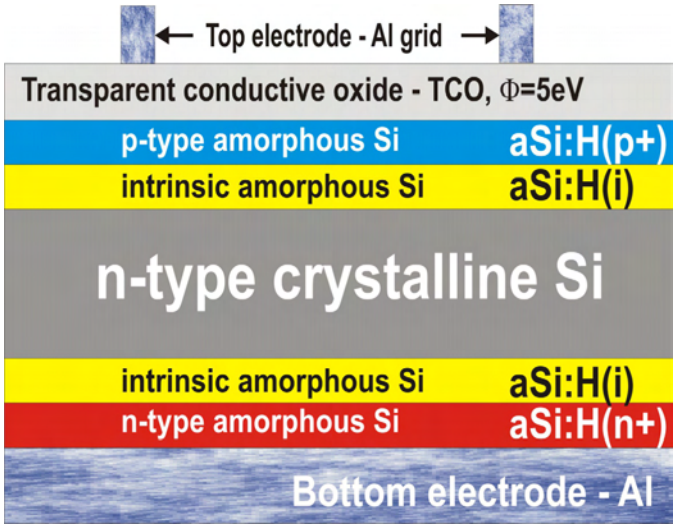

Fig. 1. HIT solar cell structure with the intrinsic amorphous Si layer.

This paper presents the results for the technology process flow and electrical characteristics of HIT solar cells simulation. Program ATHENA [4] is used for the simulation of complete production flow, while the electrical characteristics of HIT solar cell are simulated by program ATLAS [5]. Software tools ATHENA and ATLAS are an integral part of the Silvaco TCAD (Technology Computer-Aided Design) package. Initially, special attention was paid to the definition and analysis of interfacial and volume states impact on the electrical characteristics of HIT solar cells. Thereafter, the structures of the HIT cells are optimized, in order to gain V_{OC} and output power increase, taking into consideration the influence of a-Si:H(p^+) layer thickness and the level of n-type crystalline silicon supstrate doping.

II. Structure of HIT Solar Cell

The cross-section structure of HIT solar cell with a-Si:H(i) layer between the p^+ doped amorphous silicon and c-Si(n^+) from the front, and n^+ doped amorphous silicon cathode and c-Si(n^+) on the back side of solar cells is shown in Fig. 1 [6]. The TCO (transparent conductive oxide) is deposited on the front side (but it could be on both sides to provide a low serial

[1]Autors are with the Faculty of Electronic Engineering, Aleksandra Medvedeva 14, 18000 Nis, Serbia, E-mail: dragan.pantic@elfak.ni.ac.rs.
[2]Danijela Pantić is with ETŠ,"Nikola Tesla", Aleksandra Medvedeva 18, 18000 Nis, Serbia, E-mail: danijela.pantic@etstesla.ni.ac.rs.
[3]Branimir Đorđević is with the Megatrend University, Belgrade E-mail: drbranimir@gmail.com

resistance of cathode contact). An aluminum grid is deposited on the upper surface, the first electrode, and the bottom surface is aluminum metallization as a second electrode. However, the standard HIT solar cells do not have a-Si:H(i) which reduces the thickness of a-Si:H, but this layer increases the quantum efficiency of the structure, especially in the smaller wave lengths, without significant impact on the value of voltage V_{OC}. The doping profile distribution in the whole simulation domain of the HIT solar cell was obtained after simulation of the complete technology process flow by using the program ATHENA.

III. Parameters of Physical Model

To be able to simulate the electrical characteristics of HIT solar cells correctly and accurately, it is necessary to select and define properly the parameters of the physical models. This primarily refers to the definition of contacts, and to a model of the carriers generation and recombination, both in amorphous and mono-crystalline silicon, and finally the interfaces that exist in the HIT solar cell structure.

In defining the upper anode contact, it is necessary to choose carefully the material with its workfunction (*WF*), higher than 5eV. Another parameter that significantly affects the characteristics is the doping level of n-type Si crystalline layer. Less resistance, that is, higher doping ($>10^{15}$cm^{-3}) increases the value of V_{OC}, until serial resistance R_S is activated, not only due to the presence of interface states (the electronic equivalent is a parallel resistance R_P), but also due to decrease of the depletion region width, which reduces the absorption “surface” (the depletion region length).

The influence of *WF* on the HIT solar cell electrical characteristcs deals over Schottky-contact on the anode, i.e. contact potential. Klaassen's mobility model are used for the simulation, while the values of electron and hole mobilities in n^+ and p^+ a-Si:H silicon layers are μ_e=10cm^{2}V^{-1}s^{-1} and μ_h=2cm^{2}V^{-1}s^{-1}. In addition to the standard SRH, Auger and modified surface recombination model, it is necessary to define the acceptor-like and donor-like states, both at the a-Si/c-Si interface. The carriers’ lifetime τ_n and τ_p are also a function of defect energy states in the bandgap.

As already mentioned, disordered materials contain a large number of defect states within the band gap of the material. To accurately model device such as HIT solar cell, which has layers of amorphous silicon, the DEFECT statement is used to specify the density of defect states (DOS) as a combination of exponentially decaying band tail states and Gaussian distributions of mid-gap states [7] in a-Si:H and c-Si regions, and on the interfaces a-Si/c-Si.

It is assumed that the total density of states (DOS) *g(E)*, is composed of four bands: two tail bands (a donor-like valence band and an acceptor-like conduction band) and two deep level bands (one acceptor-like and the other donor-like) which are modeled using a Gaussian distribution.

$$g(E) = g_{TA}(E) + g_{TD}(E) + g_{GA}(E) + g_{GD}(E) \qquad (1)$$

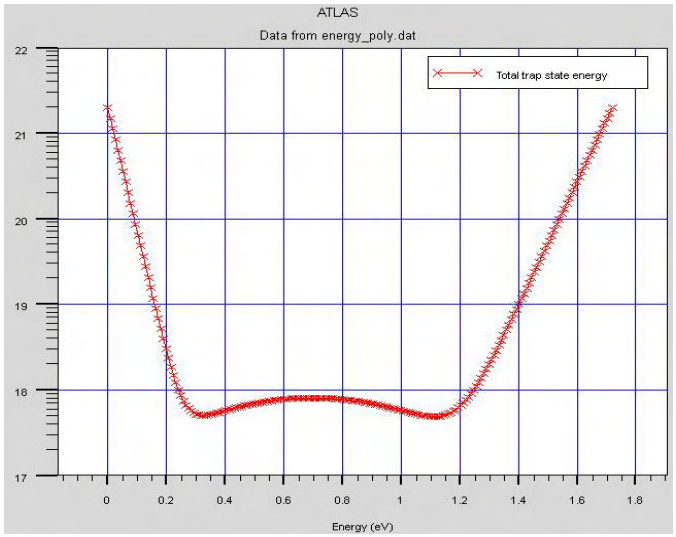

Fig. 2. The total distribution of energy states g(E) in amorphous silicon layers

The profile of energy distribution, shown on Fig. 2, has standard "U" profile. Exponential band "tail" defined for acceptor-like states and donor-like states are:

$$g_{TA}(E) = NTA \exp\left(\frac{E - E_C}{WTA}\right) \qquad (2)$$

$$g_{TD}(E) = NTD \exp\left(\frac{E_V - E}{WTD}\right) \qquad (3)$$

NTA and *NTD* are the maximum of acceptor-like and donor-like trap densities (band tail density of states), respectively (*NTA*=*NTD*=2.E+21cm^{-3}eV^{-1}). E_C is the conduction band energy, E_V is the valence band energy, while *WTA* and *WTD* are characteristic decay energy for acceptors and donors (*WTA*=0.03eV, *WTD*=0.06eV). The mid-gap traps described by Gaussian distributions of donor-like states and acceptor-like states are:

$$g_{GD}(E) = NGD \exp\left[-\left(\frac{E - EGD}{WGD}\right)^2\right] \qquad (4)$$

$$g_{GA}(E) = NGA \exp\left[-\left(\frac{EGA - E}{WGA}\right)^2\right] \qquad (5)$$

NGD and *NGA* are Gaussian maximum energy density of states in the Si doped layer (*NGD*=8.E+17cm^{-3} and *NGA*= 5.E+20cm^{-3}), while for the intrinsic Si layer *NGD*=8E+15cm^{-3} and *NGA*=5.E+17cm^{-3}. Parameters *EGD* and *EGA* are the Gaussian peak energies (*EGD*=1.22eV and *EGA*=0.7eV). The standard deviation for these functions are *WGD*=*WGA*= 0.23eV.

Capture cross-sections for the exponential "tail" distributions are *SIGTAE*=1.E-17 and *SIGTAH*=1.E-15 for the acceptor traps, and *SIGTDE*=1.E-15 and *SIGTDH*=1.E-17 for the donor traps. Electron and hole capture cross-section for

acceptor-like states of Gaussian distributions are *SIGGAE* =1.E-15, *SIGGAH*=1E-14, while for Gaussian distributions of donor-like states capture cross-sections are *SIGGDE*=1E-14 and *SIGGDH*=1E-15. These values are taken as default and they are the same for c-Si region, and also for a-Si/c-Si interface. The surface concentration of interface fixed charge is $QF=10^{10}\text{cm}^{-2}$, while the surface recombination velocity of electrons and holes are *S.N* = *S.P* =1E+3cm/s. Modeling was carried out for the life-time of carriers on the interface surface a-Si/c-Si, which is described in equations for the electrons and holes lifetimes:

$$\frac{1}{\tau_n^{eff}} = \frac{1}{\tau_n^i} + \frac{d_i}{A_i} S.N \tag{6}$$

$$\frac{1}{\tau_p^{eff}} = \frac{1}{\tau_p^i} + \frac{d_i}{A_i} S.P \tag{7}$$

where τ^i is the time specified for semiconductors bulk, and A_i and D_i are the length and area of influence for each analyzed point.

IV. Simulation Results and Discussion

The simulated HIT solar cell has two intrinsic amorphous layers on both sides of n-type mono-crystal silicon, where both of them are 10nm thick. The bulk itself is an n-type silicon. Phosphours concentration is changed in the range from $3.E+15\text{cm}^{-3}$ to $1.E+17\text{cm}^{-3}$. The doped amorphous silicon top layer a-Si:H(p+) is also a 10nm thick, doped with boron, where the doping concentration is $3E+19\text{cm}^{-3}$. The simulation results and experimental measurements showed that this concentration is a limit value for which the efficiency of HIT solar cells enters saturation. The lower doped amorphous silicon layer a-Si:H(n+) is doped with phosphorus, where the doping concentration is $1E+19\text{cm}^{-3}$. Anode electrode is 80nm thick TCO-type, while the cathode contact is made of aluminum. During the simulation it is taken into account the possible reflection of light from the lower electrode. For simulation under illumination it was used the standard AM 1.5 normalized to 0.1W/cm^2 or 100mWcm^{-2} (1sun), the wavelength vary from 0.25μm to 2.4μm. In this way the excitation of solar insolation for terrestrial systems is positioned.

As already mentioned, the workfunction value for TCO electrodes significantly affects on the open circuit voltage V_{OC} and thus on the efficiency of HIT solar cells. It is therefore important to perform the analysis of its influence.The values of *WF* are changed and the simulated output electrical characteristics for *WF* = 4.9eV, 5.1eV, 5.3eV and 5.5eV, and output power are shown in Fig. 3 and Fig. 4, respectively.

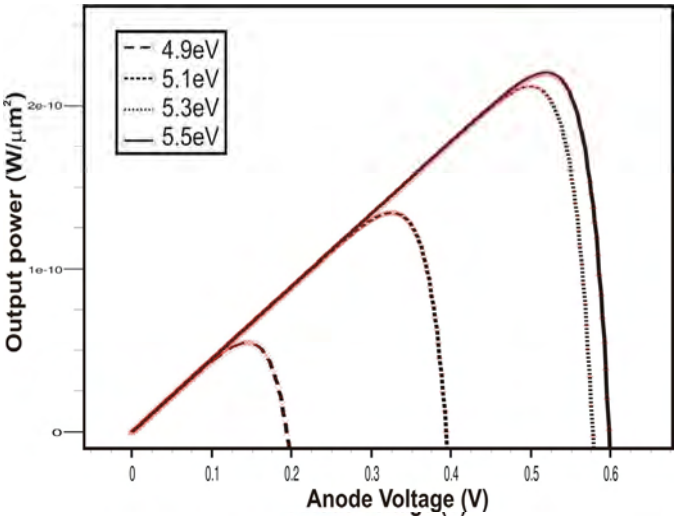

Fig. 3. I-V characteristics of HIT solar cells for different values of the parameter WF

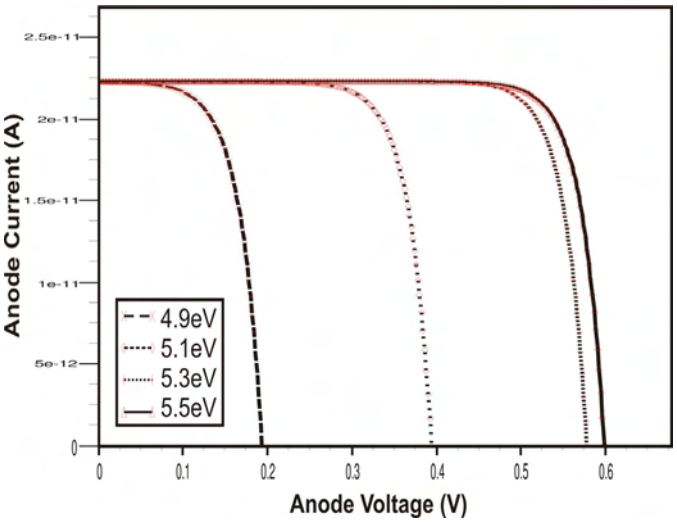

Fig. 4. Output power per μm^2 of HIT solar cell for different values of the parameter WF

Based on the simulation results it is obvious that for the *WF* values less than 5.3eV, the open circuit voltage V_{OC} rapidly changing and decreasing, while for the larger *WF* values V_{OC} saturates. The maximum value of V_{OC} = 0.6V is obtained for the *WF* = 5.5eV. For example, when the doping level of mono-crystalline Si is 1.E+16 and *WF*=5.5eV, the efficiency of HIT solar cell η=22% is obtained. It should be noted that the actual technology processes used for HIT solar cell production can make the TCO electrode with the indicated value of *WF*.

The next parameter that proved to be very important for HIT solar cell electrical characteristics is the level of mono-crystalline silicon doping. The influence of this concentration is two-fold, at least when viewed from the basic parameters. The first is the serial resistance reduction until the mobility of carriers is significantly reduced, increasing the V_{OC}, and the second is the influence on the width of the depletion region. Also, as a side effect, the relationship between the impurity concentration and interface traps could be observed.

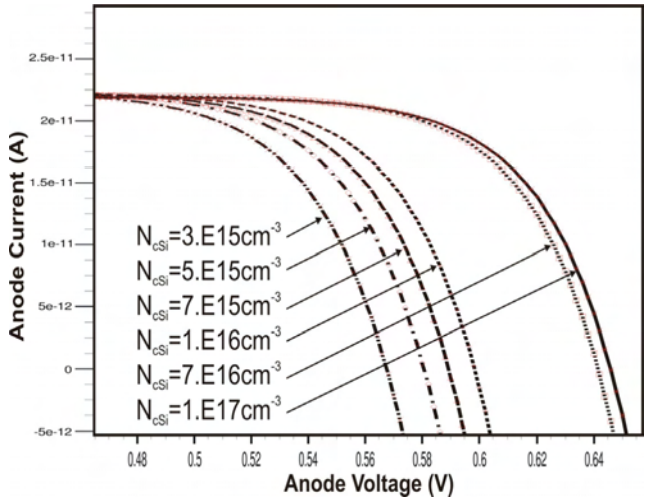

Fig. 5. Dependence of V_{OC} on doping concentration of c-Si

In Fig. 5 the dependence of V_{OC} due to doping concentration of c-Si changing is shown and V_{OC} saturation is noticed when the doping is greater than 1E+17cm^{-3}. The decrease of I_{SC} with increasing the substrate doping level can also be observed. Fig. 6 shows the dependence of output power *P*. In addition, in order to determine the coefficient of efficiency in % it is needed only to multiply the maximum value from the graphics to 10^{12} (take the absolute value).

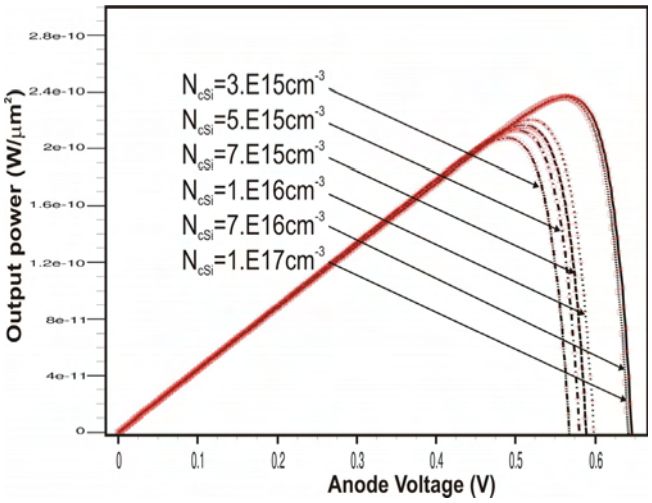

Fig. 6. Dependence of output power P (W/μm^2) on doping concentration of c-Si

Besides the saturation of the V_{OC} there is also the saturation in the HIT solar cell efficiency η. For the optimum doping level value 7.E+16cm^{-3}, gives V_{OC}=0.64V, η=23.6% and *FF*=83.48%. With further doping level increase the open circuit voltage slowly begins to decline, while the short circuit current starts to decrease significantly.

V. Conclusion

This work presents the results of simulation and optimization of the technology flow, and electrical characteristics of HIT solar cells. For the simulation of technological processes of production, ATHENA software was used, while the electrical characteristics were simulated in ATLAS software. ATHENA and ATLAS programs are an integral part of the Silvaco TCAD (Technology Computer-Aided Design) software package. It is shown that the proper choices of physical model parameters are: mobility, generation and recombination, as well as defining the contacts, and the interface can successfully and accurately simulate the electrical characteristics of HIT solar cells. The structure with the best characteristics in terms of V_{OC} and efficiency η was obtained by optimizing the most important parameters of HIT structure: the level of doping and layers thickness.

Acknowledgement

This work is partially supported by the Serbian Ministry for Education and Science under the projects TR-33035.

References

[1] S. Taira, Y. Yoshimine, T. Baba, M. Taguchi, H. Kanno, T. Kinoshita, H. Sakata, E. Maruyama, M. Tanaka, Our approaches for achieving HIT solar cells with more than 23% efficiency, in: *Proceedings of the 22nd European Photovoltaic Solar Energy Conference*, Milan, Italy, 3–7 September 2007, pp. 932–935

[2] Y. Tsunomura , Y. Yoshimine, M. Taguchi, T. Kinoshita, H. Kanno, H. Sakata, E. Maruyama, M. Tanaka, *22%-Efficiency HIT solar cell*, SANYO Electric Co., sep. 2007.

[3] L. Zhao, C.L. Zhou, H.L. Li, H.W. Diao and W.J. Wang, Design optimization of bifacial HIT solar cells on p-type silicon substrates by simulation, *Sol. Energy Mater. Sol. Cells* **92** (2008), pp. 673–681.

[4] *ATLAS User's Manual* – Device Simulation Software, SILVACO, Santa Clara, USA, 2009.

[5] *ATHENA User's Manual* – Process Simulation Software, SILVACO, Santa Clara, USA, 2009.

[6] N. Hernández-Como**,** A. Morales-Acevedo, *Simulation of hetero-junction silicon solar cells with AMPS-1D*, Solar Energy Materials and Solar Cells, Volume 94, Issue 1, Jan. 2010, pp. 62-67

[7] Kemp, A.M., M. Meunier, and C.G. Tannous, "Simulations of the Amorphous Silicon Static Induction Transistor", Solid-State Electronics, Vol. 32, No. 2 (1989): pp. 149-157.